

Neutron single particle strengths from the (d, p) reaction on ^{18}F

R. L. Kozub,¹ D. W. Bardayan,² J. C. Batchelder,³ J. C. Blackmon,² C. R. Brune,⁴ A. E. Champagne,⁵ J. A. Cizewski,⁶ U. Greife,⁷ C. J. Gross,² C. C. Jewett,⁷ R. J. Livesay,⁷ Z. Ma,⁸ B. H. Moazen,¹ C. D. Nesaraja,^{1,2} L. Sahin,^{5,9} J. P. Scott,^{1,2} D. Shapira,² M. S. Smith,² and J. S. Thomas⁶

¹*Department of Physics, Tennessee Technological University, Cookeville, Tennessee 38505, USA*

²*Physics Division, Oak Ridge National Laboratory, Oak Ridge, Tennessee 37831, USA*

³*Oak Ridge Associated Universities, Building 6008, P. O. Box 2008, Oak Ridge, Tennessee 37831-6374, USA*

⁴*Department of Physics and Astronomy, Ohio University, Athens, Ohio 45701, USA*

⁵*Department of Physics and Astronomy, University of North Carolina, Chapel Hill, North Carolina 27599, USA*

⁶*Department of Physics and Astronomy, Rutgers University, Piscataway, New Jersey 08854-8019, USA*

⁷*Department of Physics, Colorado School of Mines, Golden, Colorado 80401, USA*

⁸*Department of Physics and Astronomy, University of Tennessee, Knoxville, Tennessee 37996, USA*

⁹*Department of Physics, Dumlupinar University, Kutahya, Turkey 43100*

(Received 9 February 2006; published 12 April 2006)

The ^{19}F nucleus has been studied extensively. However, there have been no comprehensive experimental studies of $^{18}\text{F}+n$ single-particle components in ^{19}F , and no measure of neutron vacancies in the ^{18}F ground state, as such experiments require a (radioactive) ^{18}F target or beam. We have used the $^2\text{H}(^{18}\text{F},p)^{19}\text{F}$ reaction to selectively populate states in ^{19}F that are of $^{18}\text{F}+n$ character. The 108.5-MeV radioactive $^{18}\text{F}^{+9}$ beam was provided by the Holifield Radioactive Ion Beam Facility at Oak Ridge National Laboratory. Proton-recoil coincidence data were taken for both α -decaying and particle-stable final states. Angular distributions and spectroscopic factors were measured for nine proton groups, corresponding to 13 states in ^{19}F . The results are compared to shell model calculations.

DOI: [10.1103/PhysRevC.73.044307](https://doi.org/10.1103/PhysRevC.73.044307)

PACS number(s): 21.10.Jx, 25.60.Je, 25.45.Hi, 27.20.+n

I. INTRODUCTION

The structure of ^{19}F has been studied extensively, both experimentally [1] and theoretically [2,3]. This nucleus and its isospin mirror (^{19}Ne) are well known to be highly deformed systems ($\beta_2 \simeq 0.5$), with $K^\pi=1/2^+$ and $1/2^-$ rotational band heads nearly degenerate near the ground state. Various proton single-particle strength measurements for ^{19}F have been summarized recently by Terakawa *et al.* [4], including their own study of the $^{18}\text{O}(d, n)^{19}\text{F}$ reaction. However, there have been no comprehensive experimental studies of the $^{18}\text{F}+n$ character of ^{19}F levels reported previously. Such measurements are needed to specify the wave functions for excited states of ^{19}F and for the ^{18}F ground state so that nuclear structure models can be further tested. These measurements require a radioactive ^{18}F beam (or target), and ^{18}F beams have only recently become available with sufficient energy resolution and intensity for such experiments to be feasible.

In addition to enhancing our knowledge of nuclear structure, there are important astrophysical issues that can be probed in transfer reaction experiments. Indeed, an important goal of this work was to search for analogs of resonances in the ^{19}Ne mirror nucleus that could be important for the destruction of ^{18}F via the (p, γ) and (p, α) reactions in nova explosions. The relatively long half-life of the ^{18}F radionuclide (110 min) means that γ rays from electron-positron annihilation following the β^+ decay of ^{18}F would be produced after the expanding nova envelope becomes transparent to the 511-keV radiation. This should allow measurements of the abundance of ^{18}F to be made using existing and proposed gamma ray observatories, and such measurements may provide

insights about nova mechanisms. Proton resonances near the $^{18}\text{F}+p$ threshold (6411 keV) are the most interesting at nova temperatures, and a number of them seem to be “missing” in ^{19}Ne based on our knowledge of the ^{19}F mirror [1]. States having a strong $^{18}\text{F}+n$ character, such as the 6497-keV ^{19}F state seen in the present study, may be mirror analogs of some of these missing resonances. Our results for this state and other states of astrophysical significance were reported in an earlier paper [5].

II. EXPERIMENTAL PROCEDURE

A schematic diagram of the experimental setup is shown in Fig. 1. A $160(10) \mu\text{g}/\text{cm}^2$ $(\text{CD}_2)_n$ target of 98% enrichment was bombarded for ~ 3 d with an isotopically pure, 108.49 MeV $^{18}\text{F}^{+9}$ beam at an intensity of $\sim 5 \times 10^5/\text{s}$. The beam was produced at the Holifield Radioactive Beam Facility (HRIBF) at Oak Ridge National Laboratory (ORNL) as described in Ref. [6]. Using a silicon strip detector array (SIDAR) [6] of $\sim 500 \mu\text{m}$ thickness, light charged particles were detected at 16 laboratory angles in the range 118° – 157° , corresponding to “forward” center-of-mass angles in the range 8° – 27° at 7 MeV excitation in ^{19}F . The beam energy was selected to be high enough for direct reaction models, yet low enough to allow all the protons to be stopped in the SIDAR. A silicon strip detector at the focal plane of the Daresbury Recoil Separator (DRS) [7] was used to detect particle-stable recoils having $A = 19$ in coincidence with the SIDAR. This coincidence efficiency was essentially 100% of the $+9$ charge state fraction for recoil angles $< 1.6^\circ$, and $> 70\%$ overall

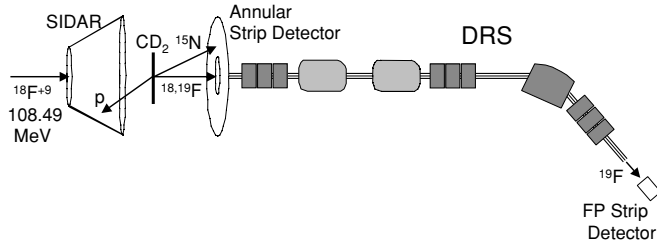


FIG. 1. Experimental setup for ${}^2\text{H}({}^{18}\text{F},p){}^{19}\text{F}$ reaction study (not to scale).

for particle-stable final states. Other recoils, from higher, α -decaying states in ${}^{19}\text{F}$, were detected in coincidence just downstream from the target with an annular strip detector. This detector was also used for data normalization. Beam current normalization was achieved by directly counting beam particles at low intensity with a retractable silicon surface barrier detector placed temporarily at 0° . The overall uncertainty in normalization, estimated to be $\sim 10\%$, is owing mostly to uncertainty in target thickness.

III. RESULTS AND ANALYSIS

Singles and coincidence spectra from the SIDAR are shown in Fig. 2 for a laboratory angle of 147° . An independent internal energy calibration was obtained for each of the 16 observed laboratory angles by using excitation energies of the well-known levels at 1.554038(9), 4.377700(42), and 5.1066(9) MeV in ${}^{19}\text{F}$ [1] (see Fig. 2). This provided up to 16 independent measurements of excitation energies up to ~ 8 MeV. The overall uncertainties are ~ 10 keV, and all the energies are consistent with known levels in ${}^{19}\text{F}$, as indicated in Table I. In addition, two relatively strong groups were observed in the coincidence data at 9.58(2) and 10.50(2) MeV excitation (not shown in Fig. 2), the latter being just above the neutron emission threshold (10.432 MeV).

Angular distributions were extracted from the singles data for all observed proton groups, and distorted-wave Born approximation (DWBA) calculations were performed with the code DWUCK5 [8] using several sets of optical model and bound state parameters from the literature. However, there seems to be a general lack of parameter families available for this mass region, a problem which is compounded by the fact that ${}^{19}\text{F}$ has a strong prolate deformation (Ref. [1] and references therein). Using “standard” values for radius and diffuseness parameters resulted in generally good fits to higher lying $3/2^+$ and $1/2^+$ states with just an $\ell = 0$ ($2s_{1/2}$) calculation, even though $\ell = 2$ transfers are also possible since the ${}^{18}\text{F}$ ground state has $J^\pi = 1^+$. However, the $\ell = 0$ component of the ground state group, which (like no other ℓ transfer) rises very steeply at forward angles, was fit very poorly with these “standard” parameters. Thus, for this work, we have used optical model and bound state parameters from Barrows *et al.* [9], who studied the ${}^{19}\text{F}(d,n){}^{20}\text{Ne}$ reaction at several bombarding energies. In Ref. [9], searches were done on these parameters to provide a best fit to the actual (d,n) reaction data. This exercise produced good fits over a wide angular

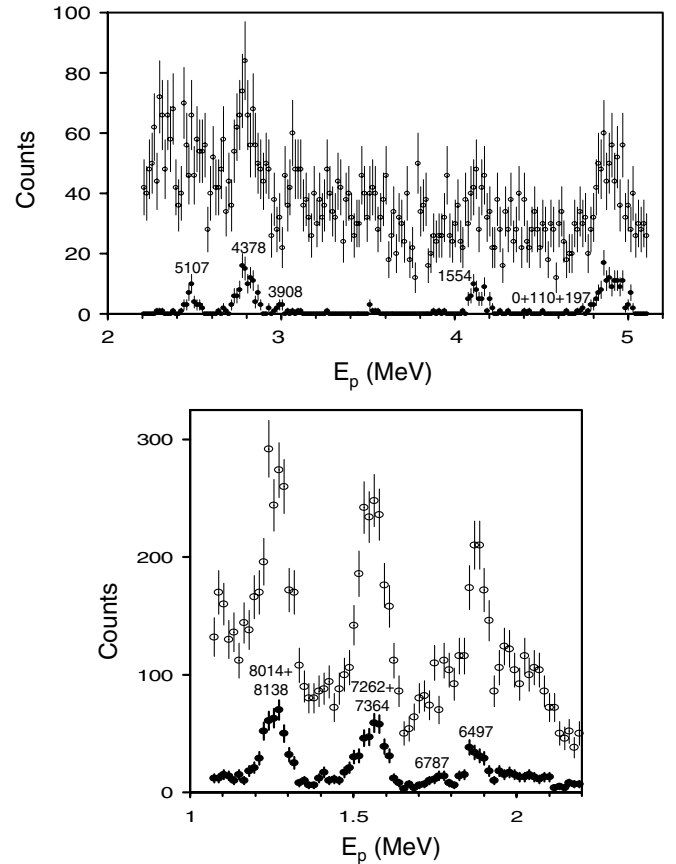


FIG. 2. Combined spectra from the six SIDAR strips corresponding to 147° lab angle as a function of proton energy, displayed in 15-keV bins. Open points are singles data ($\times 2$) while solid points ($\times 1$) are events in coincidence with the DRS focal plane detector (top spectrum) or annular strip detector (bottom spectrum). All labeled peaks followed kinematics consistent with the ${}^2\text{H}({}^{18}\text{F},p){}^{19}\text{F}$ reaction. Excitation energies are shown in keV.

range for $\ell = 0$ and $\ell = 2$ transitions, and the spectroscopic factors were quite reasonable. The resulting radius parameters were significantly larger than those normally used for spherical nuclei, but perhaps this is not an unreasonable way to treat reaction calculations for deformed systems when the direct reaction code is limited to spherically symmetric potentials. We have performed DWBA calculations for our (d, p) data using the parameters of Ref. [9] for their highest bombarding energy (6.065 MeV). These parameters are given in Table II. This resulted in good fits to our data over the 0–8 MeV range of excitation energies, including the $\ell = 0$ component of the ground state, and in reasonable spectroscopic factors (see Table I). Owing to a high background at low proton energies in the SIDAR spectra, singles angular distributions could not be extracted for the 9.58- and 10.50-MeV levels.

Since $J^\pi = 1^+$ for the ${}^{18}\text{F}$ ground state, more than one angular momentum transfer is allowed for a given final state. Indeed, with the DWBA parameters of Ref. [9], including both $\ell = 0$ and $\ell = 2$ components improves the fits at larger angles in the distributions for some of the $3/2^+$ and $1/2^+$ states, although the $\ell = 2$ curves are rather featureless over

TABLE I. Summary of data for levels observed in the ${}^2\text{H}({}^{18}\text{F},p){}^{19}\text{F}$ reaction. Uncertainties in experimental spectroscopic factors are due to curve fitting and data normalization only. Except as noted, excitation energies and J^π assignments are from Ref. [1].

Ref. [1]	${}^{19}\text{F } E_x$ (keV)		J^π	S_n^a			S_n^b			${}^{19}\text{Ne } E_x$ (keV)
	$d({}^{18}\text{F},p)^a$	OXBASH ^b		$1p_{1/2}$	$1d_{5/2}$	$2s_{1/2}$	$2p_{3/2}$	$1d_{5/2}$	$2s_{1/2}$	
0 ^c		0	$1/2^+$			0.45(9)			0.56	0
110 ^c			$1/2^-$	0.60(12)						275
197 ^c		99	$5/2^+$		0.24(5)			0.29		238
1554 ^d		1698	$3/2^+$		0.60(12)			0.77		1536
3908	3916 (10)	6627	$3/2^+$		0.2(1)			0.084		4033
4378 ^d		4871	$7/2^+$		0.30(6)			0.22		4379
5107 ^d		6373	$5/2^+$		0.15(3)			0.12		5092
6497	6497 (10)	7728	$3/2^+$		0.11(4)	0.12(2)		0.01	0.27	6419 ^f
6787	6794 (11)		$3/2^-$	0.05(1)			0.020(5)			6741 ^f
7262 ^{c,e}		8416	$3/2^+$		0.065(65)	0.16(3)		0.00	0.34	7076 ^f
7364 ^{c,e}		6084	$1/2^+$			0.16(3)			0.36	
8014 ^c		7285	$5/2^+$		0.15(3)			0.44		
8138 ^c		7819	$1/2^+$			0.32(6)			0.19	
	9580 (20)									
	10500 (20)									

^aExperimental, from the present work.

^bTheory, from Refs. [10,11].

^cMember of an unresolved group in (d, p) data.

^dUsed for energy calibration in the present work.

^eAn excitation energy of 7306(10) keV was measured in the present work for the 7262 + 7364-keV doublet.

^fSee Ref. [5] and references therein.

the angular range measured. In most cases, however, the distributions for individual levels seem to be dominated by a single ℓ transfer.

A. Triplet near the ground state

The angular distribution for the unresolved group near the ground state is shown in Fig. 3. This group contains the ground and first two excited states at 110 and 197 keV, whose spin/parity assignments are $1/2^+$, $1/2^-$, and $5/2^+$, respectively [1]. The average measured excitation energy changes with angle from ~ 30 keV for the three smallest center of mass (c.m.) angles (dominated by the $\ell = 0$ transfer to the $1/2^+$ ground state) to ~ 170 keV for the largest four angles (where the $\ell = 2$ transfer to the $5/2^+$ state is significant), indicating that at least the ground state and 197-keV state are present. However, if only those two states were present, they should have been resolved, as our c.m. resolution is ~ 120 keV. Further, the data at intermediate angles cannot be fit by using only the $\ell = 0$

and $\ell = 2$ DWBA components. Thus, we are confident that the 110-keV $1/2^-$ ‘‘intruder’’ state is also excited rather strongly, indicating significant breaking of the ${}^{16}\text{O}$ core in the ${}^{18}\text{F}$ ground state configuration [$S_n = 0.60(12)$].

TABLE II. Potential parameters used in DWBA calculations for the ${}^2\text{H}({}^{18}\text{F},p){}^{19}\text{F}$ reaction, taken from Ref. [9].

Particle	V_R (MeV)	r_R (fm)	a_R (fm)	$4V_I$ (MeV)	r_I (fm)	a_I (fm)	r_c (fm)	λ_{so}
d	109.0	1.35	0.70	58.8	1.39	0.60	1.39	
p	52.4	1.36	1.01	10.4	1.47	0.64	1.39	
n		1.46	0.73					25 ^a

^aThomas spin orbit factor; not used by Ref. [9].

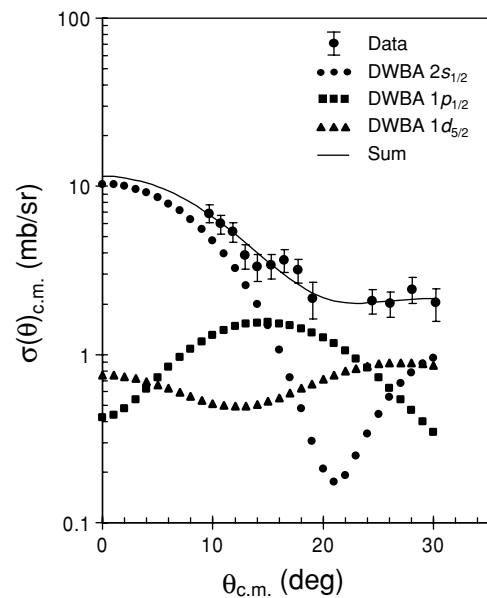


FIG. 3. Angular distribution for (d, p) transfer to the ground ($1/2^+$), 110-keV ($1/2^-$), and 197-keV ($5/2^+$) states in ${}^{19}\text{F}$. Only statistical errors are shown. Curves are DWBA calculations using parameters from Ref. [9], normalized by eye to the data. See text for details.

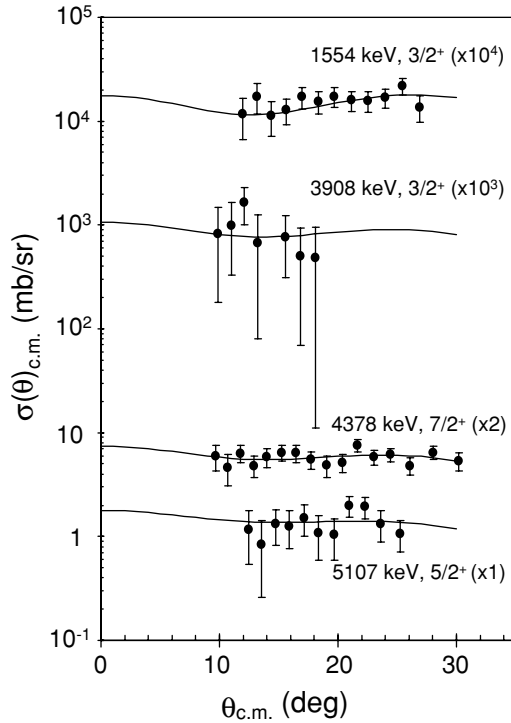


FIG. 4. Angular distributions for $\ell = 2$ (d , p) transfers to states in ^{19}F . Curves are $1d_{5/2}$ DWBA calculations. See also Fig. 3 caption.

B. $\ell = 2$ levels

Levels in ^{19}F having J^π of $3/2^+$, $5/2^+$, and $7/2^+$ can be populated via neutron transfers to the $1d_{5/2}$ orbital. The only other ℓ value that might be expected is $\ell = 0$ in the case of $3/2^+$ states, and any such contribution is easily distinguishable by the sharp rise at small center-of-mass angles. Transfers to the $1g_{7/2}$ or $1g_{9/2}$ orbitals are not expected in such a light nucleus, and the (d , p) cross section for these would be very small in any case. Given these properties, we observe four states that seem to be excited via $\ell = 2$ primarily (Fig. 4). As illustrated in Fig. 4, both the experimental and calculated angular distributions are rather featureless over the angular range measured. Some of the statistical errors are large, owing to the high background in the singles data. However, since the spins and parities are known for all these states, it is still possible to extract spectroscopic factors. These are listed in Table I. In the DWBA calculations, we have assumed all $\ell = 2$ transfers to be to the $1d_{5/2}$ orbital, as shell model calculations predict almost all of the $1d_{3/2}$ strength to lie above 9 MeV excitation energy [10]. This is a minor departure from our earlier paper [5], in which it was assumed that the $\ell = 2$ contributions in the astrophysical region corresponded to $1d_{3/2}$ transfers. However, the conclusions of that paper are not affected, since the astrophysical reaction rates are dominated by the $\ell = 0$ properties of the resonances in ^{19}Ne . It is possible that some of the $1d_{3/2}$ strength is contained in the aforementioned 9.58- and 10.50-MeV states.

C. $\ell = 0, 1$, and 2

In the bottom spectrum of Fig. 2 there are three peaks that have strong $\ell = 0$ components (6497, 7262+7364, and

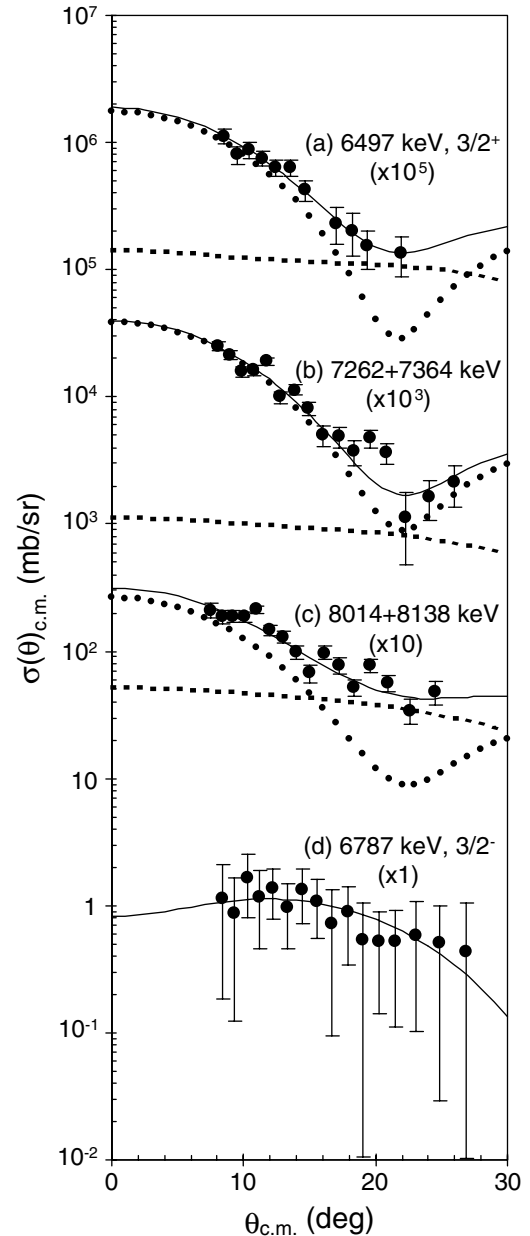


FIG. 5. Angular distributions for (d , p) transfers to states in ^{19}F . Data for states at 6497 and 6787 keV are shown in graphs (a) and (d), respectively. Graphs (b) and (c) are angular distributions for unresolved doublets at 7.3 and 8.1 MeV excitation, respectively. Dotted curves for (a), (b), and (c) are $2s_{1/2}$ calculations, dashed curves are $1d_{5/2}$ calculations, and solid curves are sums of these. A $2p_{3/2}$ calculation for (d) is shown as a solid curve. See Fig. 3 caption and text for further details.

8014+8138 keV) and one that seems to have a pure $\ell = 1$ character (6787 keV). The angular distributions and DWBA calculations for these four groups are shown in Fig. 5. The 6497-keV peak in Fig. 2 is quite narrow, and our measured excitation energy of 6497(10) keV agrees very well with that of the known $3/2^+$ level at this energy [1], so we believe this peak consists primarily of that single state.

The 7262 + 7364 peak is relatively broad, indicating that it contains more than one unresolved level. We measure an excitation energy of 7306(10) keV for this group, intermediate between known states at 7262 and 7364 keV, which have J^π of $3/2^+$ and $1/2^+$, respectively. We could detect no change in apparent excitation energy with angle for this group, so it would appear that their angular distributions are very similar, both dominated by $\ell = 0$ (Fig. 5). A two-peak fitting analysis indicates a yield ratio of $\sim 2:1$, suggesting roughly equal $2s_{1/2}$ spectroscopic factors of 0.16(3) (Table I). A small $1d_{5/2}$ contribution is included for the 7262-keV level (not possible for the 7364-keV, $1/2^+$ state). Possible mirror assignments in ^{19}Ne for the 6497- and 7262-keV levels are listed in the last column of Table I and discussed in Ref. [5].

The 8014 + 8138 peak is also broad and appears to be a combination of known states at 8014 and 8138 keV, which have J^π of $5/2^+$ and $1/2^+$, respectively. Our measured average excitation energy for this group is about 8.10 MeV for the seven smallest c.m. angles, and about 8.04 MeV for the larger angles. Here, if one assumes an absence of $1d_{3/2}$ transfers, the $\ell = 0$ and 2 components must each be totally attributed to just one of the states, i.e., to the $1/2^+$ and $5/2^+$ state, respectively. The variation of measured excitation energy with angle is consistent with this assumption, and our DWBA calculations were performed accordingly.

The remaining angular distribution in Fig. 5 is for the known $3/2^-$ state at 6787 keV. As expected, it appears to be a rather pure $\ell = 1$ distribution, but it is not clear whether the transfer is to a $1p_{1/2}$ orbital [$S_n = 0.05(1)$], to a $2p_{3/2}$ orbital [$S_n = 0.020(5)$], or to some combination thereof. In Table I, we have entered the spectroscopic factors for both the $1p_{1/2}$ and $2p_{3/2}$ possibilities.

IV. COMPARISON TO SHELL MODEL

Shell model calculations using an $(sd)^3$ model space have been performed by Brown [10] with the code OXBASH [11]. The results are listed in Table I. The agreement between experiment and theory is quite good for many of the low-lying positive parity states, e.g., the ground state and the 197-, 1554-, 4378-, and 5107-keV levels. For other states, the correspondence between experimental and calculated levels is not clear.

In the 0–8 MeV region of excitation studied here, the number of $1/2^+$, $3/2^+$, and $5/2^+$ states observed corresponds to the number of strong states predicted by the shell model in each case. In addition to the observed $7/2^+$ state at 4378 keV, two more $7/2^+$ states are predicted to be strongly excited via $1d_{5/2}$ transfer (at 5900 and 6297 keV excitation). However, we were unable to extract reliable cross section data from any more states. Perhaps these $\ell = 2$ states would be more in evidence if a (d, p) study were done at a higher bombarding energy than the present work.

For a given ℓj orbital, the number of neutron vacancies in the ^{18}F ground state is given by the quantity

$$N_{\ell j} = \sum_f \frac{2J_f + 1}{2J_i + 1} S_n(\ell, j, J_f). \quad (1)$$

TABLE III. Experimental and theoretical neutron vacancies in ^{18}F , including all levels shown in Table I except the 6787-keV level. Uncertainties in experimental numbers are due to curve fitting and data normalization only and do not include reaction model ambiguities.

$n\ell j$	$N_{\ell j}$ (Present work)	$N_{\ell j}$ (Theory)
$1p_{1/2}$	0.40(8)	0.41 ^a
$1d_{5/2}$	3.18(31)	3.44 ^b
$2s_{1/2}$	0.99(9)	1.55 ^b

^aReference [12].

^bReference [10].

Here, J_i is the spin of the initial nucleus ($=1$ here), J_f is the spin of the final state, and $S_n(\ell, j, J_f)$ is the spectroscopic factor. The experimental and calculated vacancies are summarized in Table III. The agreement is quite reasonable for the $1d_{5/2}$ orbital, especially when one considers reaction model ambiguities. However, the calculated vacancy in the $2s_{1/2}$ orbital is about 50% higher than experiment. This is probably owing to the $(sd)^3$ restriction on the model space, which does not include the significant vacancy in the $1p_{1/2}$ orbital. Our measured value of 0.40(8) for the $1p_{1/2}$ vacancy is in excellent agreement with the total vacancy of 0.41 extracted from the ^{18}F ground state wave function published by Zuker [12], although it is somewhat surprising that essentially all of this strength is contained in one state. Clearly, a shell model calculation with the model space expanded to include the $1p_{1/2}$ shell would be very interesting.

V. SUMMARY

In summary, using the $^2\text{H}(^{18}\text{F}, p)^{19}\text{F}$ reaction, we have measured neutron spectroscopic factors for 13 levels in ^{19}F , 12 for the first time [13]. In order to fit the $\ell = 0$ ground state angular distribution for this deformed system, it was necessary to use optical and bound state potentials with unusually large radius parameters. For low-lying states, shell model calculations using an $(sd)^3$ model space are in good agreement with experiment for transfers to the $1d_{5/2}$ orbital, while predictions for $2s_{1/2}$ transfers are about 50% too large. However, our results show evidence for significant breaking of the ^{16}O core in the ground state of ^{18}F , so new calculations which include the $1p_{1/2}$ orbital in the model space are needed. Finally, as discussed in Ref. [5], there are some unresolved issues involving analog assignments for states at higher excitations in the ^{19}F - ^{19}Ne mirror pair which can only be clarified by proton transfer experiments. A measurement at the HRIBF to address this issue, using the $^2\text{H}(^{18}\text{F}, ^{15}\text{O}\alpha)n$ reaction, has been conducted recently [14].

ACKNOWLEDGMENTS

Thanks are owed to the staff of the HRIBF for making this experiment possible, to D. J. Dean for valuable discussions, and to B. A. Brown for performing the shell model calculations. This work is supported in part by

U.S. DOE Grant Nos. DE-FG02-96ER40955 (TTU) and DE-FG02-93ER40789 (CSM) and by the National Science

Foundation (RU). ORNL is managed by UT-Battelle, LLC, for the U.S. DOE under Contract No. DE-AC05-00OR22725.

-
- [1] D. R. Tilley, H. R. Weller, C. M. Cheves, and R. M. Chasteler, *Nucl. Phys.* **A595**, 1 (1995).
- [2] J. B. McGrory and B. H. Wildenthal, *Phys. Rev. C* **7**, 974 (1973).
- [3] B. A. Brown, B. H. Wildenthal, C. F. Williamson, F. N. Rad, S. Kowalski, Hall Crannell, and J. T. O'Brien, *Phys. Rev. C* **32**, 1127 (1985).
- [4] A. Terakawa *et al.*, *Phys. Rev. C* **66**, 064313 (2002).
- [5] R. L. Kozub *et al.*, *Phys. Rev. C* **71**, 032801(R) (2005).
- [6] D. W. Bardayan *et al.*, *Phys. Rev. C* **63**, 065802 (2001).
- [7] R. Fitzgerald *et al.*, *Proceedings of the 6th International Conference Radioactive Nuclear Beams* [*Nucl. Phys.* **A748**, 351 (2005)].
- [8] P. D. Kunz, University of Colorado (unpublished).
- [9] A. W. Barrows, Jr., F. Gabbard, and J. L. Weil, *Phys. Rev.* **161**, 928 (1967).
- [10] B. A. Brown (private communication) (2005).
- [11] B. A. Brown, A. Etchegoyen, N. S. Godwin, W. D. M. Rae, W. A. Richter, W. E. Ormand, E. K. Warburton, J. S. Winfield, L. Zhao, and C. H. Zimmerman, NSCL Report No. 524.
- [12] A. P. Zuker, *Phys. Rev. Lett.* **23**, 983 (1969).
- [13] See N. de Séréville *et al.*, *Phys. Rev. C* **67**, 052801(R) (2003); N. de Séréville, E. Berthoumieux, and A. Coc, *Proceedings of the 8th International Symposium of Nuclei in the Cosmos* [*Nucl. Phys.* **A758**, 745 (2005)].
- [14] C. R. Brune *et al.*, abstract L8.00004 at APS April Meeting (2006); see also <http://www.phy.ornl.gov/hribf/news/feb06/brune.shtml>.